

Communication

(E)-1-(4-Ethoxycarbonylphenyl)-5-(3,4-dimethoxyphenyl)-3-(3,4-dimethoxystyryl)-2-pyrazoline: Synthesis, Characterization, DNA-Interaction, and Evaluation of Activity Against Drug-Resistant Cell Lines

Dimitris Matiadis ¹, Barbara Mavroidi ¹, Angeliki Panagiotopoulou ¹, Constantinos Methenitis ², Maria Pelecanou ¹ and Marina Sagnou ^{1,*}

¹ National Center for Scientific Research “Demokritos”, Institute of Biosciences & Applications, 153 10 Athens, Greece; matiadis@bio.demokritos.gr (D.M.); bmavroidi@bio.demokritos.gr (B.M.); apanagio@bio.demokritos.gr (A.P.); pelmar@bio.demokritos.gr (M.P.)

² National and Kapodistrian University of Athens, Department of Chemistry, 157 84 Athens, Greece; methenitis@chem.uoa.gr.

* Correspondence: sagnou@bio.demokritos.gr; Tel.: +30-210-6503558

Received: 15 January 2020; Accepted: 27 January 2020; Published: 30 January 2020

Abstract: (E)-1-(4-Ethoxycarbonylphenyl)-5-(3,4-dimethoxyphenyl)-3-(3,4-dimethoxystyryl)-2-pyrazoline was synthesized via the cyclization reaction between the monocarbonyl curcuminoid (2E,6E)-2,6-bis(3,4-dimethoxybenzylidene)acetone and ethyl hydrazinobenzoate in high yield and purity (>95% by High-performance liquid chromatography (HPLC)). The compound has been fully characterized by ¹H, ¹³C NMR, FTIR, UV-Vis and HRMS and its activity was evaluated in terms of its potential interaction with DNA as well as its cytotoxicity against resistant and non-resistant tumor cells. Both DNA thermal denaturation and DNA viscosity measurements revealed that a significant intercalation binding takes place upon treatment of the DNA with the synthesized pyrazoline, causing an increase in melting temperature by 3.53 ± 0.11 °C and considerable DNA lengthening and viscosity increase. However, neither re-sensitisation of Doxorubicin (DOX)-resistant breast cancer and multidrug resistance (MDR) reversal nor synergistic activity with DOX by potentially increasing the DOX cell killing ability was observed.

Keywords: pyrazolines; curcuminoids; nitrogen heterocycles; cytotoxic; DNA binding; MDR reversal

1. Introduction

Nitrogen-containing heterocycles are important core structures found in many natural products [1] and synthetic compounds exhibiting a broad range of biological activities. Recent analysis of a Food and Drug Administration-approved drug database revealed that 59% of unique small-molecule drugs contain at least one nitrogen heterocycle [2]. Pyrazolines in particular, constitute a class of five-membered heterocycles incorporating a nitrogen-nitrogen (N-N) bond [3], with remarkable pharmacological applications [4] as anticancer [5–9], anti-inflammatory [10–12], antimicrobial [13,14], and antimalarial drugs [15].

Representative examples of synthetic bioactive pyrazolines are depicted in Figure 1. Thiazolone containing pyrazoline **1** has been found to be selectively active against colon cancer cell lines, especially on HT-29 [6]. Benzimidazole pyrazoline **2** has been reported by Shaharyar et al. as the most active antitumor compound among a library of selected similar derivatives [7], whereas benzenesulfonamide pyrazoline **3** was shown by Rathish et al. in in vitro and in vivo studies to be a

more potent anti-inflammatory agent than celecoxib [10]. Manna et al. investigated 1-acetyl-3,5-diaryl-pyrazolines **4a** and **4b** for their anticancer activity and binding affinity to P-glycoprotein [16]. On the other hand, 3,5-divinylpyrazole **5** (Figure 1) which is a curcumin derivative, has been reported by Kolotova et al. as a potent inhibitor of P-glycoprotein, which is associated with the induction of multidrug resistance in cancer chemotherapy [17,18]. Such molecules have consequently caused resensitisation of the resistant cells and reversal of the multidrug resistance phenomenon [18]. Taking into account the aforementioned promising findings, we synthesized compound **6** (Figure 2) which is the pyrazoline analogue of the curcuminoid pyrazole derivative **5**, and we studied its interaction with DNA as well as its cytotoxicity against chemo-resistant and non-resistant tumor cells.

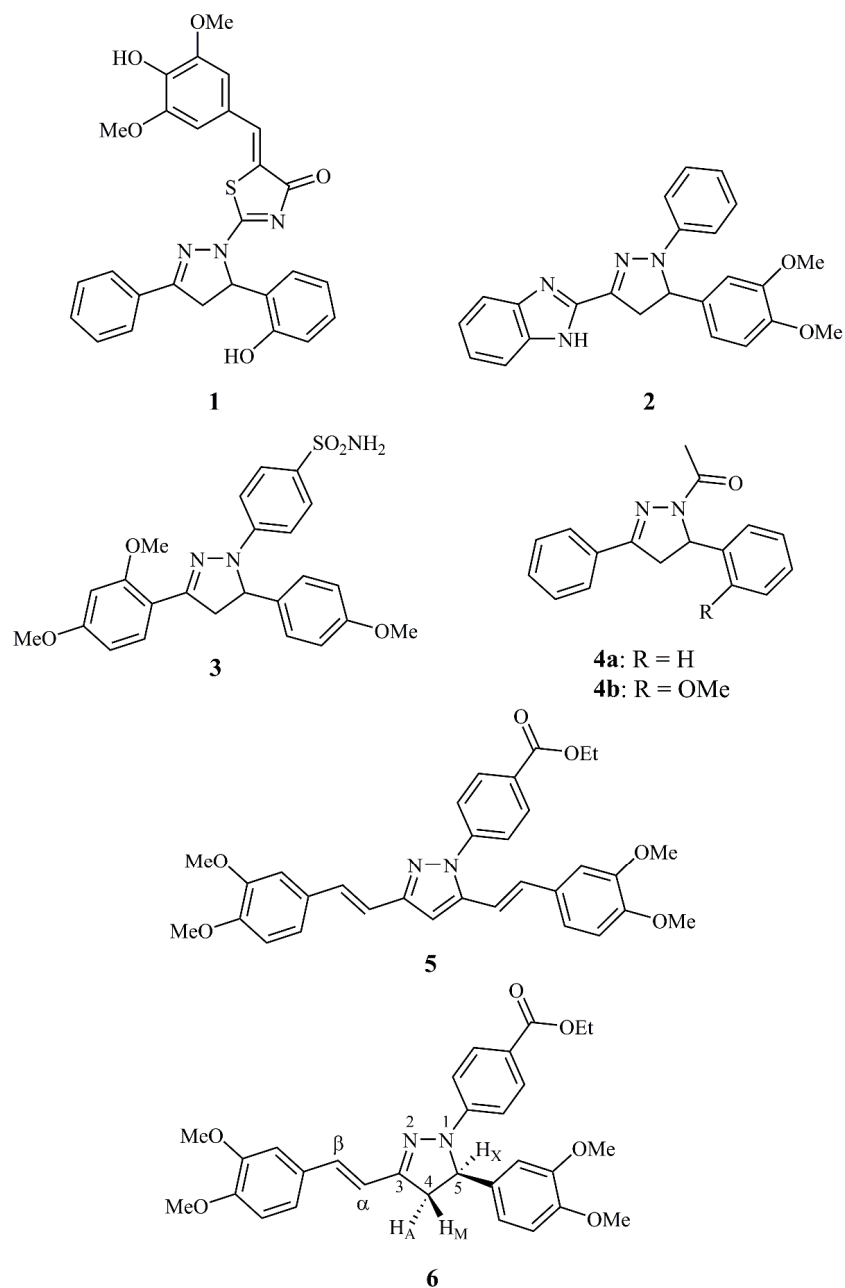
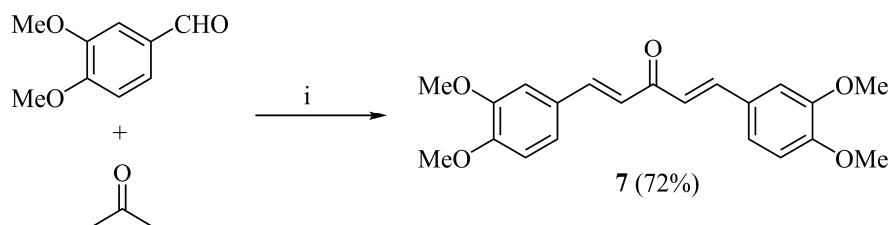


Figure 1. Structures of known biologically active pyrazolines **1–4**, pyrazole **5** and title pyrazoline **6**. The numbering of compound **6** skeleton is according to common pyrazoline nomenclature. The product **6** is racemic, however the relative configuration is shown for clarity and simplicity purposes to describe the AMX system and the assignments.

2. Results and Discussion

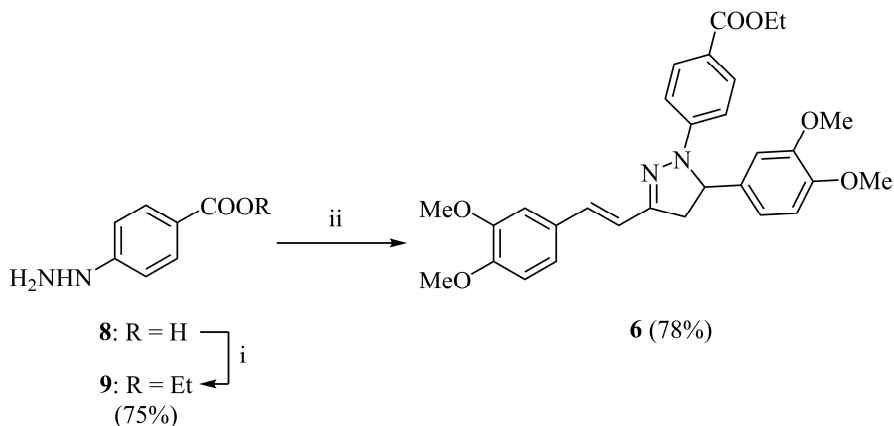
2.1. Synthesis and Characterization

The synthetic route towards the preparation of the title compound **6** is outlined in Schemes 1 and 2. In the first step, the intermediate symmetrical monocarbonyl curcuminoid **7** was synthesized from acetone and veratraldehyde via base-catalyzed Claisen–Schmidt condensation reaction and used after recrystallization from ethanol (Scheme 1).



Scheme 1. Synthesis of monocarbonyl curcuminoid intermediate **7**. Reagents and conditions: (i) NaOH, EtOH, 2 h, r.t.

In the second step, **7** reacted with ethyl hydrazinobenzoate **9**, prepared from the esterification of the corresponding carboxylic acid **8** with ethanol and concentrated sulfuric acid. The cyclization reaction between curcuminoid **7** and the hydrazine **9** in refluxing glacial acetic acid afforded the desired pyrazoline **6** in high yield and purity without the need for further purification. However, for analytical or biological purposes, even higher purity was achieved by ethanol precipitation ($\geq 95\%$), as determined by high performance liquid chromatography (HPLC, see Supplementary Materials)



Scheme 2. Synthesis of (*E*)-1-(4-ethoxycarbonylphenyl)-5-(3,4-dimethoxyphenyl)-3-(3,4-dimethoxyphenyl)-2-pyrazoline **6**. Reagents and conditions: (i) H₂SO₄, EtOH, reflux, 5 h; (ii) **7**, glacial AcOH, reflux, 5 h.

The structure of **6** has been confirmed by NMR spectroscopy and HRMS spectrometry. The characteristic signals assigned to the protons on C-4 (H_M, H_A) and C-5 (H_X) of the pyrazoline ring (Figure 1) can be described as a typical AMX spin system. Three doublets of doublets appear at 3.03 (H_A), 3.78 (H_M) and 5.51 (H_X) ppm. The coupling constants conform to this abovementioned pattern having the following *J* values: *J*_{AM} = 17.2 Hz the *J*_{AX} = 4.6 Hz for the *cis*- configuration and *J*_{MX} = 12.2 Hz for the *trans*. Moreover, the large *J* value (16.4 Hz) of the vinylic H_α and H_β protons, appearing at 6.81 and 7.21 ppm respectively, is in accordance with the expected *E*-configuration of the double bond. The rest of the ¹H signals, along with the ¹³C signals, were assigned by means of 2D NMR (COSY, HSQC and HMBC—see Supporting material).

The FTIR spectrum of the prepared compound further supports the formation of a 2-pyrazoline. The characteristic C=N and C-N bonds of the molecule appear at 1600 and 1250 cm⁻¹ respectively as

strong bands, while the medium intensity band at 1700 cm^{-1} is assigned to the C=O of the aromatic ester.

2.2. Biological Evaluation

2.2.1. DNA Binding Studies

The potential of compound **6** to interact with CT-DNA was studied by means of the biophysical methods of DNA melting and DNA viscosity changes. Firstly, in thermal denaturation experiments for CT-DNA alone, under our experimental conditions, a T_m of $69.02 \pm 0.31\text{ }^\circ\text{C}$ was recorded, a value that is in good agreement with reported literature values [19]. Upon co-incubation of increasing concentrations of compound **6** with CT-DNA ($5 \times 10^{-5}\text{ M}$), a concentration-dependent rise of T_m values was recorded reaching a ΔT_m value of $3.53 \pm 0.11\text{ }^\circ\text{C}$ at the highest [compound **6**]/[DNA] ratio of $R = 0.5$ (Figure 2A). As in the literature an increase in melting temperature with ΔT_m values ranging from $+3\text{ }^\circ\text{C}$ to $+14\text{ }^\circ\text{C}$ is associated with intercalative binding [20], the observed ΔT_m value suggests that compound **6** may interact with DNA through intercalation. To further investigate the nature of this interaction with CT-DNA, viscosity measurements were carried out. In general, interaction of a compound with DNA results in changes in the length of DNA [21]. When classical intercalation occurs, DNA lengthening is usually observed, due to the separation of base pairs at the intercalation site, which produces a concomitant increase in the relative specific viscosity of such solutions. As it is shown by the viscosity data obtained (Figure 2B), with increasing concentration of compound **6**, the relative viscosity of CT-DNA increases continuously, providing additional evidence of intercalation mode of binding. Curcumin and curcumin derivatives are known to interact with DNA via groove binding [22–25], as demonstrated by UV-visible, competitive fluorescence studies, CD spectroscopy, DNA viscosity and melting studies. The interaction of the pyrazoline curcuminoid **6**, with DNA via the intercalative mode, demonstrates the fact that structural modifications of bioactive molecules modulate dramatically their mechanism, mode and specificity of action.

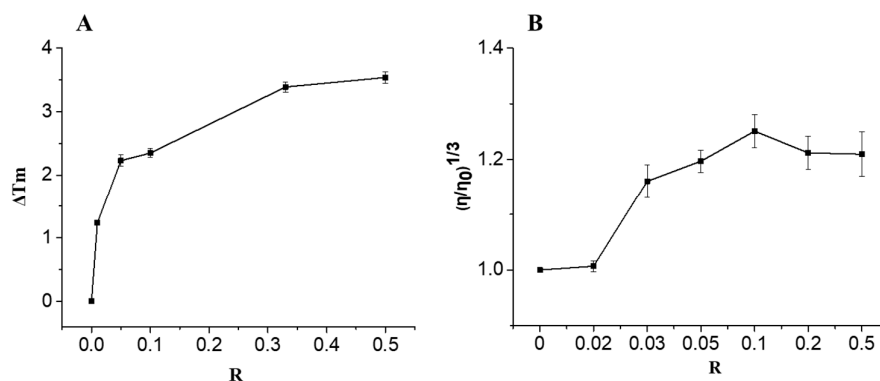


Figure 2. Thermal denaturation data of CT-DNA (A) and Effect of increasing amounts on the relative viscosity of CT-DNA (B) upon addition of compound **6** with ratios $R = [\text{compound } 6]/[\text{DNA}]$ ranging from 0 to 0.5.

2.2.2. In Vitro Cytotoxicity Studies Against Doxorubicin-Resistant Breast Cancer Cells

To assess the relative toxicity of compound **6**, Doxorubicin (DOX) and their combination, the MTT colorimetric method was employed against MCF-7 breast cancer cell line and the corresponding DOX-resistant (MCF-7/DOX^R) cell line. Compound **6** exhibited moderate toxicity against both MCF-7 DOX-sensitive and resistant cells, with IC_{50} values of $53.09\text{ }\mu\text{M}$ and $85.11\text{ }\mu\text{M}$ respectively, following a 48 h treatment (Table 1). Furthermore, the IC_{50} value obtained for the cytotoxicity of DOX in MCF-7 was in good agreement with literature data [26], and as expected, in the MCF-7/DOX^R cells DOX was found to be less toxic compared to corresponding non-resistant cells

(14-fold lower). In order to evaluate the potential ability of compound **6** to re-sensitize the DOX-resistant cells and re-establish a low IC₅₀ value for DOX, or investigate the potential synergistic activity of compound **6** with DOX in the parental cell line, both the MCF-7 and the MCF-7/DOX^R cells were pre-treated with a small amount of compound **6** before the DOX co-incubation. As presented in Table 1, compound **6** did not alter IC₅₀ values of DOX in either cell lines and no significant reduction was observed. Our data reveal that even though compound **6** has a close structural similarity with **5** it does not seem to reverse drug resistance in DOX-resistant MCF-7/DOX^R and re-sensitize them as well as no synergistic activity was exhibited with DOX against the parental MCF-7 cells.

Table 1. Effect of curcuminoid pyrazoline **6** on DOX sensitivity in MCF-7 and MCF-7/DOX^R.

Compound	IC ₅₀ (μM)	
	MCF-7	MCF-7-DOX ^R
6	53.09 ± 3.58	85.11 ± 4.68
DOX	5.22 ± 1.33	70.90 ± 8.75
DOX (pre-incubated with 6)	7.71 ± 1.59	72.55 ± 4.99

3. Materials and Methods

3.1. General

All reagents were purchased from Sigma-Aldrich (St. Louis, MO, USA) and Alfa Aesar (Lancaster, UK) unless otherwise stated and used without further purification. All the media/agents for the cultures of cells were purchased from Thermo Fisher Scientific (Cleveland, OH, USA). Melting points were determined with a Gallenkamp MFB-595 melting point apparatus (Weiss Gallenkamp, London, UK). NMR spectra were recorded with a Bruker Avance 500 MHz spectrometer (Bruker, Rheinstetten, Germany) operating at 500 MHz (¹H) and 125 (¹³C). Chemical shifts are reported in ppm relative to DMSO-*d*₆ (¹H: δ = 2.50 ppm, ¹³C: δ = 39.52 ± 0.06 ppm) or CDCl₃ (¹H: δ = 7.26 ppm). UV-Vis spectra were recorded with a Hitachi U-3010 spectrophotometer (Hitachi, Tokyo, Japan). IR spectra were recorded on a Perkin-Elmer Spectrum 100-IR spectrophotometer (Perkin-Elmer, San Francisco, CA, USA). HRMS spectra were recorded on UHPLC LC-MSn Orbitrap Velos-Thermo instrument (Thermo Scientific; Bremen, Germany) in the Institute of Biology, Medicinal Chemistry and Biotechnology of the National Hellenic Research Foundation. HPLC analysis was performed with a Waters 600E Chromatography System coupled with a Waters 486 UV detector (at 254 nm) (Waters, Manchester, UK). Separation was achieved on a C-18 reverse phase column (250 × 4 mm, 5 μm) eluted with a binary gradient system at 1 mL/min flow rate. Mobile phase A was methanol containing 0.1% trifluoroacetic acid, while mobile phase B was water containing 0.1% trifluoroacetic acid. The elution gradient was 0–1 min 5% A (95% B), followed by a linear gradient to 70% A (30% B) in 5 min; this composition was held for another 3 min; 85% A (15% B) for 17 min. After a column wash with 95% A (5% B) for 10 min, the column was re-equilibrated by applying the initial conditions 5% A (95% B) for 10 min prior to the next injection.

3.2. (1*E*,4*E*)-1,5-Bis(3,4-dimethoxyphenyl)penta-1,4-dien-3-one (**7**)

To a solution of veratraldehyde (3.32 g, 20 mmol) and acetone (0.98 g, 10 mmol) in ethanol (10 mL) was added a suspension of NaOH (5 g, 125 mmol) in ethanol (40 mL). The resulting suspension was stirred for 2 h at room temperature. After 10 min, a yellow solid started to precipitate. The mixture was filtered, washed with water (×3) and dried. The resulting solid was recrystallized from ethanol to afford the product as yellow needles (2.84 g, 7.20 mmol, 72%). Mp: 79–80 °C; ¹H NMR (500 MHz, DMSO-*d*₆): δ 3.82 (s, 6H, OMe), 3.84 (s, 6H, OMe), 7.03 (d, *J* = 8.3 Hz, 2H, Ph), 7.23 (d, *J* = 15.9 Hz, 2H, -CH=CH-Ph), 7.33 (d, *J* = 8.3 Hz, 2H, Ph), 7.40 (s, 2H, Ph), 7.70 (d, *J* = 15.9 Hz, 2H, -CH=CH-Ph) [27–29].

3.3. Ethyl 4-hydrazinobenzoate (9)

To a solution of 4-hydrazinobenzoic acid (1.52 g, 10 mmol) in absolute ethanol (20 mL) was added dropwise concentrated H₂SO₄ (1 mL). After stirring under reflux for 8 h, the mixture was cooled to room temperature and then concentrated under vacuum. The residue was suspended in AcOEt (40 mL) and washed with a saturated K₂CO₃ solution. The latter was extracted two times with AcOEt (20 mL). The combined organic solutions were dried over Na₂SO₄ and the solvent was evaporated to afford the product as off-white solid (1.35 g, 7.5 mmol, 75%). Mp: 106–107 °C; ¹H NMR (500MHz, CDCl₃): δ 1.37 (t, *J* = 7.0 Hz, 3H, CH₃CH₂), 3.31 (br, 2H, NHNH₂), 4.33 (q, *J* = 7.0 Hz, 2H, CH₃CH₂), 5.52 (br, 1H, NHNH₂), 7.40 (d, *J* = 7.4 Hz, 2H, Ph), 7.92 (d, *J* = 7.4 Hz, 2H, Ph) [30].

3.4. (E)-1-(4-Ethoxycarbonylphenyl)-5-(3,4-dimethoxyphenyl)-3-(3,4-dimethoxystyryl)-2-pyrazoline (6)

A mixture of the curcuminoid **7** (177 mg, 0.50 mmol) and ethyl 4-hydrazinobenzoate **9** (270 mg, 1.50 mmol) was refluxed in glacial acetic acid (6 mL) for 5 h. The solution was cooled to 50 °C and then poured into ice-cold water (50 mL). The completion of the reaction was monitored by TLC (*n*-hexane/AcOEt = 7:3) after mini work-up. The precipitate was filtered and washed thoroughly with water (×3). The product (199 mg, 0.39 mmol, 78%) was dried in a desiccator over CaCl₂ overnight. For analytical purposes, it was precipitated from hot ethanol. Yellow solid. Mp: 76–77 °C; UV-Vis (EtOH) λ_{max} (log ε): 388 nm (4.65); FTIR (KBr, cm⁻¹): 1700, 1600, 1510, 1265, 1170, 1105, 1025, 765; ¹H NMR (500 MHz, DMSO-*d*₆): δ 1.26 (t, *J* = 6.8 Hz, 3H, CH₃CH₂O-), 3.03 (dd, *J*_{MX} = 4.6 Hz, *J*_{AM} = 17.1 Hz, 1H, CH_AH_M), 3.69 (s, 3H, MeO), 3.71 (3H, s, MeO), 3.74 (dd, *J*_{AX} = 11.8 Hz, *J*_{AM} = 17.1 Hz, 1H, CH_AH_M), 3.77 (s, 3H, MeO), 3.81 (s, 3H, MeO), 4.21 (q, *J* = 6.8 Hz, 2H, CH₃CH₂O-), 5.51 (dd, *J*_{MX} = 4.6 Hz, 1H, *J*_{AX} = 11.8 Hz, CH_X), 6.65 (d, *J* = 7.8 Hz, 1H, Ph), 6.81 (d, *J* = 16.2 Hz, 1H, H_β), 6.87 (1H, s, Ph), 6.88 (d, *J* = 7.8 Hz, 1H, Ph), 6.94 (d, *J* = 8.4 Hz, 1H, Ph), 6.99 (d, *J* = 8.6 Hz, 2H, Ph), 7.08 (d, *J* = 8.4 Hz, 1H, Ph), 7.21 (d, *J* = 16.2 Hz, 1H, H_α), 7.26 (s, 1H, Ph), 7.74 (d, *J* = 8.6 Hz, 2H, Ph); ¹³C NMR (125 MHz, DMSO-*d*₆): δ 14.3 (CH₃CH₂), 42.0 (C-4), 55.46 (2C, CH₃O-), 55.48 (2C, CH₃O-), 59.8 (CH₃CH₂), 61.8 (C-5), 109.2 (CH-arom), 109.5 (CH-arom), 111.7 (CH-arom), 112.0 (2C, CH-arom), 112.2 (CH-arom), 117.3 (CH-arom), 118.8 (C_α), 120.8 (CH-arom), 129.2 (2C, C_q-arom), 130.6 (2C, CH-arom), 134.0 (C_q-arom), 135.1 (C_β), 146.9 (C_q-arom), 148.1 (C_q-arom), 149.0 (C_q-arom), 149.1 (C_q-arom), 149.4 (C_q-arom), 151.9 (C-3), 165.6 (-COOEt); HRMS: calcd for C₃₀H₃₃N₂O₆ (M⁺ + H) 517.2333; found 517.2328; HPLC: *t*_R = 16.5 min.

3.5. Preparation of DNA Samples

All DNA experiments were performed in phosphate buffer (0.05 M, pH = 7.2) consisting of Na₂HPO₄ and KH₂PO₄. The CT-DNA solution was sufficiently free of protein as evidenced by the ratio of its UV absorbance at 260 and 280 nm that was approx. 1.9:1 [20]. The DNA concentration per nucleotide was determined spectrophotometrically by using the molar absorption coefficient of ε = 6600 M⁻¹·cm⁻¹ per nucleotide at 260 nm. Before each measurement, fresh stock solutions of CT-DNA and compound **6** (in DMSO at a concentration of 10⁻³ M) were prepared and the corresponding mixtures were incubated for 24 h at 25 °C to reach the equilibrium state. Each reported measurement value is the average of three independent experiments.

3.6. Thermal Denaturation Studies

DNA melting temperature measurements were performed using a Varian Cary 300 spectrophotometer (Agilent Technologies, Inc., Santa Clara, CA, USA) equipped with a heating multiple cell block apparatus. Temperatures were maintained under computer control and were increased at a 0.5 °C/min rate. DNA melting experiments were carried out by monitoring the absorbance of DNA at 258 nm in the temperature range from 25.0 °C to 95.0 °C. Solutions were allowed to equilibrate for 1 min at each temperature. Cuvettes (1.0 cm capped quartz) were mounted in a thermal block and the solution temperatures were monitored by a thermistor in the reference cuvette. The melting temperature (*T*_m) of DNA was determined as the midpoint of the optically detected transition and the measurement was repeated three times for each sample. The melting

experiments were performed in phosphate buffer solution (final percentage of DMSO = 2%) by keeping the DNA concentration constant (5×10^{-5} M) while varying the concentration of compound **6** ($0 - 2.5 \times 10^{-5}$ M) to achieve ratios $R = [\text{compound } 6]/[\text{DNA}]$ of 0, 0.01, 0.05, 0.1, 0.33, 0.5.

3.7. Viscosity Studies

Viscosity measurements were carried out using Ostwald's viscometer (Schott geräte, type 531 01/0a, thermostat Schott geräte GT 1150, meter Schott geräte AVS 300) at 25 °C (Schott –Instruments GmbH, Germany). The viscometer was thermostated at 25.0 ± 0.1 °C in a constant temperature bath. Flow time of solutions was measured with a digital stopwatch and each sample was measured three times and an average flow time was calculated. The values did not differ by more than 0.2 s from each other. All solutions were filtered through 0.22 µm filter (Millipore, Billerica, MA) prior to the measurements. Experiments were carried out in phosphate buffer solution (final percentage of DMSO = 2%) by keeping the DNA concentration constant (5×10^{-5} M) while varying the concentration of compound **6** ($0 - 2.5 \times 10^{-5}$ M) to achieve ratios $R = [\text{compound } 6]/[\text{DNA}]$ of 0, 0.02, 0.033, 0.05, 0.1, 0.2, 0.5. The intrinsic viscosity $[\eta]$ was calculated according to the relation $[\eta] = (t - t_b)/t_b$, where t_b is the flow time for the buffer and t is the observed flow time for DNA in the presence or absence of the compound **6**. Data were presented as $(\eta/\eta_0)^{1/3}$ versus R where η and η_0 are the intrinsic viscosities in the presence or absence of the compound **6**. For the low DNA concentrations used in these experiments, the intrinsic viscosity $[\eta]$ is proportional to the difference in the flow time for the buffer with and without DNA, resulting in the following Eq. (1) [31]:

$$\frac{L}{L_0} = \frac{[\eta]^{1/3}}{[\eta_0]^{1/3}} = \frac{(t - t_b)^{1/3}}{(t_0 - t_b)^{1/3}}$$

where L and L_0 are the DNA lengths and $[\eta]$ and $[\eta_0]$ are the intrinsic viscosities with and without the compound. The t_b , t_0 and t are the flow times of the buffer, the plain DNA and the DNA/compound solution, respectively.

3.8. Cell Culture

Human breast adenocarcinoma MCF-7 cells (American Type Culture Collection, Manassas, VA, USA), were grown in DMEM growth medium of pH 7.4 supplemented with 10% FBS, 100 U/mL of penicillin, 2 mM glutamine and 100 µg/mL of streptomycin. Cell cultures were maintained in flasks and were grown at 37 °C in a humidified atmosphere of 5% CO₂ in air. Subconfluent cells were detached using a 0.25% (*w/v*) trypsin–0.03% (*w/v*) EDTA solution and the split ratio was 1:3–1:5. Doxorubicin-resistance was established by stepwise exposure of MCF-7 cells to increased concentrations of DOX ranging between 0.01 and 1 µg/mL. Finally, the MCF-7/DOX^R cells were able to grow continually in medium with 0.1 µg/mL DOX. The stock solutions of compound **6** and DOX at a concentration of 10 mM dissolved in DMSO were diluted to different concentrations as required.

3.9. In Vitro Cytotoxicity Assay

In vitro cytotoxicity of compound **6**, DOX and the combination of them against the MCF-7 and MCF-7/DOX^R cell lines was determined by the MTT colorimetric assay. Cells were seeded in 96-well plates (10^4 cells/well) and grown overnight at 37 °C in a 5% CO₂ incubator. Exponentially growing cells were incubated for 48 h with various concentrations ranging between 10^{-3} – 10^{-8} M of compound **6** and DOX and the final DMSO concentration never exceeded 0.2%. For the combination experiments, MCF-7/DOX^R cells were pre-incubated for 1 h with compound **6** (10^{-5} M) and then DOX was added in various concentrations (10^{-3} – 10^{-8} M) for another 47 h. The medium was then removed and replaced with 100 µL of MTT solution (Sigma-Aldrich, Darmstadt, Germany, 1 mg mL⁻¹). After a 4 h incubation, the solution was aspirated, formazan crystals were solubilized in 100 µL of dimethyl sulfoxide (DMSO) and absorbance was recorded at 540 nm (Tecan well plate reader, Tecan, Grödig, Austria). The results were expressed as % cell viability = (mean optical density (OD) of treated cells/mean OD of untreated cells) × 100. Data were plotted against the corresponding compound

concentration in a semi-log chart and the values of IC₅₀ (the concentration of test compound required to reduce the fraction of live cells to 50% of the control) were calculated from the dose–response curves using GraphPad Prism 5.0 software (GraphPad Software Inc, CA, USA).

4. Conclusions

(*E*)-1-(4-Ethoxycarbonylphenyl)-5-(3,4-dimethoxyphenyl)-3-(3,4-dimethoxystyryl)-2-pyrazoline was successfully synthesized for the first time from the corresponding monocarbonyl acetone-derived curcuminoid and ethyl hydrazinobenzoate in high yield and purity. The compound exhibited significant intercalation binding activity with CT-DNA, which renders it a suitable lead compound for further derivatisation aiming to improve its DNA binding capacity. However, despite its structural similarity with the corresponding curcumin pyrazoline derivative which has shown MDR reversal activity no re-sensitisation of DOX-resistant breast cancer was observed and there was no synergistic activity with DOX against non-resistant cell lines. Further investigation is underway to identify whether conversion of the pyrazoline to pyrazole moiety may improve the MDR reversal activity of such monocarbonyl curcumin derivatives.

Supplementary Materials: All the spectroscopic data of the title compound **6** namely ¹H and ¹³C NMR, ¹H-¹H COSY NMR, HSQC and HMBC NMR, FT-IR, HRMS, UV-Vis spectra, and HPLC are available online.

Author Contributions: Conceptualization, M.S.; methodology and data analysis, D.M and B.M.; 2D NMR analysis A.P. and M.P.; writing—original draft preparation, D.M., B.M. M.S.; writing—review and editing and funding acquisition, M.P.; supervision, M.S., C.M. and M.P. All authors have read and agreed to the published version of the manuscript.

Funding: The authors acknowledge financial support of this work by the project “Target Identification and Development of Novel Approaches for Health and Environmental Applications” (MIS 5002514) which is implemented under the Action for the Strategic Development on the Research and Technological Sectors, funded by the Operational Programme “Competitiveness, Entrepreneurship and Innovation” (NSRF 2014-2020) and co-financed by Greece and the European Union (European Regional Development Fund). B. Mavroidi gratefully acknowledges financial support by Stavros Niarchos Foundation (SNF) through implementation of the program of Industrial Fellowships at NCSR “Demokritos”.

Conflicts of Interest: The authors declare no conflict of interest. The funders had no role in the design of the study; in the collection, analyses, or interpretation of data; in the writing of the manuscript, or in the decision to publish the results.

References

1. Hanessian, S., Ed. *Natural products in medicinal chemistry*, Wiley-VCH: Weinheim, 2014.
2. Vitaku, E.; Smith, D. T.; Njardarson, J. T.; Analysis of the structural diversity, substitution patterns, and frequency of nitrogen heterocycles among U.S. FDA approved pharmaceuticals. *J. Med. Chem.* **2014**, *57*, 10257–10274, doi:10.1021/jm501100b.
3. Varghese, B.; Al-Busafi, S. N.; Suliman, F. O.; Al-Kindy, M. Z. Unveiling a versatile heterocycle: Pyrazoline—a review. *RSC Adv.* **2017**, *7*, 46999–47016, doi:10.1039/c7ra08939b.
4. Shaaban, M. R.; Mayhoub, A. S.; Farag, A. M. Recent advances in the therapeutic applications of pyrazolines. *Expert Opin. Ther. Patents* **2012**, *22*, 253–291, doi:10.1517/13543776.2012.667403.
5. Akhtar, J.; Khan, A. A.; Ali, Z.; Haider, R.; Yar, M. S. Structure-activity relationship (SAR) study and design strategies of nitrogen-containing heterocyclic moieties for their anticancer activities. *Eur. J. Med. Chem.* **2017**, *125*, 143–189, doi:10.1016/j.ejmech.2016.09.023.
6. Havrylyuk, D.; Zimenkovsky, B.; Vasylenko, O.; Zaprutko, L.; Gzella, A.; Lesyk, R. Synthesis of novel thiazolone-based compounds containing pyrazoline moiety and evaluation of their anticancer activity. *Eur. J. Med. Chem.* **2009**, *44*, 1396–1404, doi:10.1016/j.ejmech.2008.09.032.
7. Shaharyar, M.; Abdullah, M. M.; Bakht, M. A.; Majeed, J. Pyrazoline bearing benzimidazoles: Search for anticancer agent. *Eur. J. Med. Chem.* **2010**, *45*, 114–119, doi:10.1016/j.ejmech.2009.09.032.
8. Insuasty, B.; Montoya, A.; Becerra, D.; Quiroga, J.; Abonia, R.; Robledo, S.; Vélez, I. D.; Upegui, Y.; Nogueras, M.; Cobo, J. Synthesis of novel analogs of 2-pyrazoline obtained from

- [(7-chloroquinolin-4-yl)amino]chalcones and hydrazine as potential antitumor and antimalarial agents. *Eur. J. Med. Chem.* **2013**, *67*, 252–262, doi:10.1016/j.ejmech.2013.06.049.
9. Shin, S. Y.; Yoon, H.; Hwang, D.; Ahn, S.; Kim, D.-W.; Koh, D.; Lee, Y. H.; Lim, Y. *Bioorg. Med. Chem.* **2013**, *21*, 7018–7024, doi:10.1016/j.bmc.2013.09.014.
 10. Rathish, I. G.; Javed, K.; Ahmad, S.; Bano, S.; Alam, M. S.; Pillai, K. K.; Singh, S.; Bagchi, V. Synthesis and antiinflammatory activity of some new 1,3,5-trisubstituted pyrazolines bearing benzene sulfonamide. *Bioorg. Med. Chem. Lett.* **2009**, *19*, 255–258, doi:10.1016/j.bmcl.2008.10.105.
 11. Bansal, E.; Srivastava, V. K.; Kumar, A. Synthesis and anti-inflammatory activity of 1-acetyl-5-substitute daryl-3-(b-aminonaphthyl)-2-pyrazolines and b-(substituted aminoethyl) amidonaphthalenes. *Eur. J. Med. Chem.* **2001**, *36*, 81–92, doi:10.1016/S0223-5234(00)01179-X.
 12. Lokeshwari, D. M.; Achutha, D. K.; Srinivasan, B.; Shivalingegowda, N.; Krishnappagowda, L. N.; Kariyappa, A. K. Synthesis of novel 2-pyrazoline analogues with potent anti-inflammatory effect mediated by inhibition of phospholipase A2: Crystallographic, in silico docking and QSAR analysis. *Bioorg. Med. Chem. Lett.* **2017**, *27*, 3806–3811, doi:10.1016/j.bmcl.2017.06.063.
 13. Karthikeyan, M. S.; Holla, B. S.; Kumari, N. S. Synthesis and antimicrobial studies on novel chloro-fluorine containing hydroxy pyrazolines. *Eur. J. Med. Chem.* **2007**, *42*, 30–36, doi:10.1016/j.ejmech.2006.07.011.
 14. Siddiqui, Z. N.; Musthafa, T. N. M.; Ahmad, A.; Khan, A. U. Thermal solvent-free synthesis of novel pyrazolyl chalcones and pyrazolines as potential antimicrobial agents. *Bioorg. Med. Chem. Lett.* **2011**, *21*, 2860–2865, doi:10.1016/j.bmcl.2011.03.080.
 15. Mishra, V. K.; Mishra, M.; Kashaw, V.; Kashaw, S. K. Synthesis of 1,3,5-trisubstituted pyrazolines as potential antimalarial and antimicrobial agents. *Bioorg. Med. Chem.* **2017**, *25*, 1949–1962. h: 10.1016/j.bmc.2017.02.025.
 16. Manna, F.; Chimenti, F.; Fioravanti, R.; Bolasco, A.; Secci, D.; Chimenti, P.; Ferlini, C.; Scambia, G. Synthesis of some pyrazole derivatives and preliminary investigation of their affinity binding to P-glycoprotein. *Bioorg. Med. Chem. Lett.* **2005**, *15*, 4632–4635, doi:10.1016/j.bmcl.2005.05.067.
 17. Kolotova, E. S.; Shtil, A. A.; Novikov, F. N.; Chilov, G. G.; Stroganov, O. V.; Stroilov, V. S.; Zeifman, A. A.; Titov, I. Y.; Sagnou, M.; Alexiou, P. Novel derivatives of 3,5-divinyl-pyrazole for medical application. WO 2016/190770 A1, 01 December 2016.
 18. Gottesman, M. M.; Pastan, I.; Ambudkar, S. V. P-Glycoprotein and multidrug resistance. *Curr. Opin. Gen. Dev.* **1996**, *6*, 610–617, doi:10.1016/S0959-437X(96)80091-8.
 19. Halevas, E.; Mavroidi, B.; Swanson, C. H.; Smith, G. C.; Moschona, A.; Hadjispyrou, S.; Salifoglou, A.; Pantazaki, A. A.; Pelecanou, M.; Litsardakis, G. Magnetic cationic liposomal nanocarriers for the efficient drug delivery of a curcumin-based vanadium complex with anticancer potential. *J. Inorg. Biochem.* **2019**, *199*, 110778, doi:10.1016/j.jinorgbio.2019.110778.
 20. Mavroidi, B.; Sagnou, M.; Stamatakis, K.; Paravatou-Petsotas, M.; Pelecanou, M.; Methenitis, C. Palladium(II) and platinum(II) complexes of derivatives of 2-(4'-aminophenyl)benzothiazole as potential anticancer agents. *Inorg Chim. Acta*, **2016**, *444*, 63–75, doi:10.1016/j.ica.2016.01.012.
 21. Suh, D.; Chaires, J. B. Criteria for the mode of binding of DNA binding agents, *Bioorg. Med. Chem.* **1995**, *3*, 723–728, doi:10.1016/0968-0896(95)00053-j.
 22. Zsila, F.; Bikádi, Z.; Simonyi, M. Circular dichroism spectroscopic studies reveal pH dependent binding of curcumin in the minor groove of natural and synthetic nucleic acids, *Org. Biomol. Chem.*, **2004**, *2*, 2902–2910, doi:10.1039/B409724F.
 23. Kunwar, A.; Simon, E.; Singh, U.; Chittela, R. K.; Sharma, D.; Sandur, S. K.; Priyadarsini, I. K. Interaction of a curcumin analogue dimethoxycurcumin with DNA. *Chem. Biol. Drug Des.* **2011**, *77*, 281–287.
 24. Sahoo, B. K.; Ghosh, K. S.; Bera, R.; Dasgupta, S. Studies on the interaction of diacetylcurcumin with calf thymus-DNA. *Chem. Phys.* **2008**, *351*, 163–169, doi:10.1016/j.chemphys.2008.05.008.
 25. R. Bera, B. K. Sahoo, K. S. Ghosh and S. Dasgupta, *Int. J. Biol. Macromol.*, **2008**, *42*, 14–21.
 26. Arif, I. S.; Hooper, C. L.; Greco, F.; Williams, A. C.; Boateng, S. Y. Increasing doxorubicin activity against breast cancer cells using PPAR γ -ligands and by exploiting circadian rhythms. *Br J Pharmacol.* **2013**, *169*, 1178–1188, doi:10.1111/bph.12202.
 27. Li, Q.; Chen, J.; Luo, S.; Xu, J.; Huang, Q.; Liu, T. Synthesis and assessment of the antioxidant and antitumor properties of asymmetric curcumin analogues. *Eur. J. Med. Chem.* **2015**, *93*, 461–469, doi:10.1016/j.ejmech.2015.02.005.

28. Butcher, R. J.; Jasinski, J. P.; Yathirajan, H. S.; Bindya, S.; Narayana, B.; Sarojini, B. K. 1,5-Bis(3,4-dimethoxyphenyl)penta-1,4-dien-3-one. *Acta Cryst.* **2007**, *E63*, o3115, doi:10.1107/S1600536807026888.
29. Du, Z.-Y.; Bao, Y.-D.; Liu, Z.; Qiao, W.; Ma, L.; Huang, Z.-S.; Gu, L.-Q.; Chan, A. S. C. *Arch. Pharm. Chem. Life Sci.* **2006**, *339*, 123–128, doi:10.1002/ardp.200500205.
30. Bourrie, B.; Casellas, P.; Ciapetti, P.; Derocq, J.-M.; Jegham, S.; Muneaux, Y.; Wermuth, C.-G. Pyridoindolone derivatives substituted in the 3-position by a phenyl, their preparation and their application in therapeutics. US 7,390,818 B2, 24 June 2008.
31. Cohen, G.; Eisenber, Viscosity and sedimentation study of sonicated DNA–proflavine complexes. *Biopolymers.* **1969**, *8*, 45, doi: 10.1002/bip.1969.360080105 H., 8 (1) (1969) 45



© 2020 by the authors. Licensee MDPI, Basel, Switzerland. This article is an open access article distributed under the terms and conditions of the Creative Commons Attribution (CC BY) license (<http://creativecommons.org/licenses/by/4.0/>).